



Thermal Resistance of Fibre-Reinforced and FRP-Wrapped RC Columns: An Experimental Investigation

Maulik Mistry ^a, Prasad Barve ^a, Piyush Patel ^{a, *}

^a Applied Mechanics Department, Government Engineering College, Godhra-389001, Gujarat, India

* Corresponding Author Email: piyu27286@gmail.com

DOI: <https://doi.org/10.54392/irjmt25316>

Received: 31-01-2025; Revised: 12-04-2025; Accepted: 21-04-2025; Published: 12-05-2025



Abstract: Elevated temperatures significantly affect the construction industry, particularly for reinforced concrete (RC) columns. Although concrete resists high temperatures, exposure can cause spalling, cracking, and reduced load-bearing capacity. This study examines the effects of incorporating composite materials, such as steel, polypropylene, and hybrid fibres, into concrete and using fibre-reinforced polymer (FRP) wrapping to strengthen RC columns exposed to high temperatures. Thirty RC column specimens were cast, varying in dimensions, concrete type (control, steel fibres, polypropylene fibres, hybrid fibres reinforced), and FRP wrapping (Glass Fibre Reinforced Polymer (GFRP), Carbon Fibre Reinforced Polymer (CFRP)). The columns were subjected to 200 °C for 6 hours per day over 75 cycles and then tested for ultimate load-carrying capacity (failure load), displacement, secant stiffness, strain, failure modes, and crack patterns. The results showed that steel fibre-reinforced columns had higher failure loads than other fibre-reinforced columns. FRP-wrapped columns experienced a 7.35% to 23.36% decrease in failure load when exposed to high temperatures compared with unheated FRP-wrapped columns. Fibre-reinforced columns displayed lower displacement compared to control columns after exposure to 200 °C, whereas FRP-wrapped columns showed higher displacement. The findings recommended using various types of fibre-reinforced concrete and FRP wrapping to increase the load-carrying capacity and strengthen RC columns, particularly those exposed to high temperatures.

Keywords: High temperature, Steel fibres, Polypropylene fibres, Hybrid fibres, GFRP, CFRP

1. Introduction

Reinforced concrete (RC) columns are widely used in the construction industry due to their structural efficiency and durability. High temperatures are very influential occupational hazards, which may risk the structure and safety of RC columns in construction [1, 2]. Despite the fact that concrete has good high-temperature performance, but [3, 4] shows that too high temperature promotes the spalling of concrete, the development of cracks and reduces the load carrying capacity of RC columns. Although the data on the effect of high temperature on concrete are well-known, relatively few studies have investigated the addition of composite materials and the FRP wrapping as a means to improve the performance of RC columns under such conditions. In dealing with improving high-temperature resistance in RC columns, it is worth exploring the utilization of conventional composite materials like steel fibres, polypropylene fibres and hybrid fibres and FRP wrapping [5-9]. Indian design codes, such as IS 456:2000 and IS 1642:2013, provide comprehensive guidelines to ensure fire resistance in reinforced concrete (RC) structures. These codes specify the

minimum cover requirements, fire ratings for various structural elements, and material properties at elevated temperatures, thereby ensuring the adequate fire performance of RC buildings in India.

Many earlier studies have been published on how higher temperatures change the characteristics of concrete reinforced with various kinds of fibres. To achieve more flexural toughness, Bezerra et al. [10] suggested that steel fibre-reinforced concrete particularly showed more resistance against the impacts of increased temperatures than control concrete specimens. By adding steel fibres, concrete's mechanical qualities were maintained after three hours at 500 °C, increasing the material's structural resilience at high temperatures. Roy et al.'s study [11] examined how high-strength concrete (HSC) with polypropylene fibres behaved structurally under temperatures ranging from 25 °C to 750 °C and stated that even though it adversely affected the fresh properties, the mechanical properties improved while adding polypropylene fibre and strength loss at elevated temperatures was decreased. At elevated temperatures, an optimal ratio of

1.0 kg/m³ was determined for polypropylene fibres that maintained excellent mechanical strength of HSC.

The combined effect of steel fibres and hybrid polypropylene (PP) on preventing explosive spalling in ultrahigh-performance concrete (UHPC) at high temperatures was investigated by Li et al. [9] Due to a significant increase in permeability, their study showed that the addition of hybrid PP and steel fibres successfully inhibited explosive spalling, even at low fibre concentrations. Jianqiang et al. [12] have studied the thermal deterioration of high strength engineered cementitious composites (HSECC). According to their examination, HSECC has a lower cracking temperature threshold than ECC of normal strength; yet, explosive spalling was successfully reduced by adding 2.0 vol% PVA fibre. Despite having more severe compression failure modes, HSECC outperformed ECC in terms of decreased mass and strength loss. Banoth and Agarwal [13] found that the interphase behavior of the link between concrete and deformed steel rebars under high temperatures depends on the heating rate, and reported the comparison of flexural bond strength. Based on their findings they found that bond strength was affected more with rapid heating and the bond strength per unit surface area decreased for rebars having a larger diameter. As the contact temperature increased, the bond ductility was deteriorated faster than the bond strength. The performance of concrete under extreme heat conditions was explored by Kabashi et al. [14] who showed that the mechanical and physical properties of concrete changed with increasing of temperature. This thorough analysis provides significant new data on how concrete behaves when subjected to these extreme temperatures, vital to enhancing structural resilience across a range of applications.

Trapko [15] investigated the impact of elevated temperatures on concrete components reinforced with carbon fibre-reinforced polymers (CFRPs) and fibre-reinforced cementitious matrices (FRCM). This study examined the failure patterns and assessed the ultimate load-bearing capacity through laboratory experimentation and analytical computations. Moghtadernejad et al. [16] identified the implementation of external confinement with fibre-reinforced polymers (FRP) as a rehabilitation method for fire damaged concrete columns. The results showed that the post-heated columns strengthened with double FRP layers were significantly improved in ultimate axial load capacity compared to the non-exposed specimens. Liew et al. [17] investigated the mechanical properties of glass fibre-reinforced polymer (GFRP) material by performing tensile and flexural experiments, and then the beam reinforcement effectiveness was studied by performing four-point bending tests. This joint research contributes to a better understanding of the behavior of different concrete and reinforcement materials at elevated temperatures. The knowledge on these studies can be quite useful for increasing strength and performance of

structures in those conditions. FRP sheets are effective for strengthening heat-damaged circular RC columns but did not restore stiffness as reported by Al-Nimry and Ghanem [18]. The significance of assessing the impact of elevated temperature on column properties and the need for updating design guidelines in this field is emphasized via this investigation. Vijayan et al. [19] performed a study on the effects of wrapping the GFRP sheets (3 mm and 5 mm thickness) on rectangular columns of 150 mm × 300 mm cast in M 20 and M 40 grades. Their findings revealed that FRP-wrapped columns exhibited significantly improved axial compressive strength and Young's modulus compared to normal concrete, with 5 mm wrapping providing superior performance over 3 mm wrapping in both concrete grades. Fibre-reinforced polymer (FRP) confinement has been extensively studied for its ability to enhance the load-carrying capacity, compressive strength, and ductility of columns by Mohammad and Karim [20]. Column cross-section geometry, aspect ratio, concrete strength, FRP thickness, and wrapping technique all affect how successful FRP confinement is. When compared to their counterparts, circular columns, lower aspect ratios, weaker concrete, thicker FRP layers, and fully wrapped layouts typically show better performance advantages.

In order to assess the heat resistance and structural behavior of FRC and FRP-wrapped columns, the study focuses on 200 °C as the critical temperature. The complete melting of polypropylene fibres at this temperature creates microchannels that lower the risk of spalling and relieve internal vapor pressure [21]. Also, it is noticed that the first degradation of FRP wraps starts around 200 °C [22]. Steel fibres improve mechanical strength retention and crack-bridging capabilities [23]. By assessing the impact of different fibre types and FRP wrapping on reinforced concrete columns exposed to elevated temperatures, this investigation addresses a critical knowledge gap regarding steel, polypropylene and hybrid fibre-reinforced concrete behavior under heating conditions. Various structural parameters like ultimate load-carrying capacity (failure load), displacement, secant stiffness, strain, failure modes, and crack patterns for all RC column specimens are essential to understand the behavior of RC columns subjected to axial loading condition. Through the comparison of each of the above parameters in relation to the behavior of unheated RC columns and heated RC columns, the authors attempt to contribute to enhancing the design and safety of reinforced concrete structures in fire-susceptible environments. The findings support the development of effective strengthening techniques for enhanced structural resilience, particularly in the Indian context, where this approach is still emerging.

2. Materials and Methods

2.1 Experimental design and specimen preparation

This study investigates the effectiveness of various techniques for rehabilitating and strengthening heat-damaged reinforced concrete (RC) columns. Thirty RC columns were fabricated using M 25 grade of concrete. The experimental variables included the exposure temperature and specific reinforcement strategies (Table 1).

2.2 Concrete mixture and reinforcement

The concrete mixture comprised crushed limestone aggregate (maximum size of 20 mm) [24], natural river sand (Zone II), ordinary Portland cement [25] and potable water. Table 2 presents the concrete mix proportions [26] employed for the study.

All specimens featured consistent reinforcement designs in accordance with IS 456 specifications [27]. The longitudinal reinforcement consisted of 6 nos. of ϕ 12 mm (ϕ = diameter of bar) (Fe415 grade steel), while the lateral ties were ϕ 8 mm (Fe415 grade steel), spaced 150 mm centre-to-centre.

2.3 Fibre-reinforced concrete mixtures

The columns were casted using four concrete varieties: control (without fibre), steel fibre-reinforced, polypropylene fibre-reinforced, and hybrid fibre-reinforced. The optimal fibre concentrations for the respective mixes were determined to be 1% steel fibres and 2% polypropylene fibres per cubic meter. The hybrid composition of fibres incorporated 0.5% steel fibres and 2% polypropylene fibres per cubic metre of concrete. A concrete pan mixer with a high shear capacity was used to prepare the concrete mixture. The dry ingredients were mixed for 2-3 minutes to ensure consistent mix, and then approximately 70% water was added and mixed for another 3 minutes. Fibres were then added to the wetted concrete mix and physically observed to ensure that the fibres were evenly dispersed into the concrete. It is worth noting that no fibre aggregation was observed. The remaining water was then added to the mixture to develop homogeneous and workable fibre reinforced concrete.

2.4 Specimen casting and curing

The specimens were casted in the laboratory using steel moulds. After 24 h, the columns were extracted from the moulds and wrapped in gunny bags for curing. Water curing was continued for 28 days, after which the columns were stored under ambient temperature and humidity conditions.

2.5 Surface preparation

The concrete surface was ground using a surface-smoothing grinder to create a smooth and uniform base for FRP system applications. Minor protrusions and grouting lines were mechanically scraped, and necessary repairs were executed using a mortar. The height differential between adjacent concrete surfaces was maintained at less than 1 mm.

2.5.1 Application of primer, putty and saturant

A primer coat was applied to achieve a homogeneous surface finish as shown in Figure 1. The coating, consisting of a base and hardener in a 100:50 ratio, was applied manually, resulting in a reflective mirror-like surface. The coated surface solidified within 6 h. To level the concrete surface and remove irregularities resulting from the column casting, a layer of epoxy putty was applied. The putty consisted of two components, base and hardener, combined in a ratio of 100:75 (base: hardener) as displayed in Figure 2. The saturant, composed of a base and hardener combined in a 100:40 (base: hardener) ratio, was thoroughly blended for approximately 1 min. It was then applied to the surface using a hand brush as shown in Figure 3. The properties of primer are as depicted in Table 3, and that for the putty and saturant are presented in Table 4.

2.5.2 Fibre reinforcement system application

The fibre reinforcement system was cut into the required sizes before applying the saturant. Similar procedures were adopted for both the CFRP and GFRP composites. After applying the saturant, the fibres were wrapped around the columns to ensure a proper fibre direction for effective confinement. The fibres were pressed onto the wet saturant by hand and a roller to achieve proper bonding and remove entrapped air. Figure 4 shows the CFRP-wrapped column, whereas Figure 5 shows the GFRP-wrapped column. The properties of CFRP and GFRP are presented in Table 5.

2.6 Heating regime

From the past literature [28], the concrete specimens underwent a cyclic heating and cooling regime for a total of 75 cycles. Each cycle consisted of two phases: 1. Oven exposure: Specimens were kept in an oven at 200 °C for 6 hours. 2. Cooling period: Specimens were then allowed to cool at room temperature for 18 hours. After completing the 75 cycles, all testing was conducted at laboratory room temperature.

Table 1 Details of column specimens

Column designation	Column size		No. of specimens	Heating condition	Strengthening method
	Diameter (mm)	Height (mm)			
Unheated reinforced column (UHRC)	150	300	02	Control	-
		450	02		
Heated reinforced column (HRC)	150	300	02	Heated at 200 °C	-
		450	02		
Heated steel fibre reinforced column (HSFRC)	150	300	02	Heated at 200 °C	Steel fibres
		450	02		
Heated polypropylene fibre reinforced column (HPPFC)	150	300	02	Heated at 200 °C	Polypropylene fibres
		450	02		
Heated hybrid fibre reinforced column (HHFRC)	150	300	02	Heated at 200 °C	Hybrid fibres (Steel + Polypropylene fibres)
		450	02		
Heated GFRP wrapped reinforced column (HGWRC)	150	300	02	Heated at 200 °C	GFRP wrapped sheet
		450	02		
Heated CFRP wrapped reinforced column (HCWRC)	150	300	02	Heated at 200 °C	CFRP wrapped sheet
		450	02		
Unheated GFRP wrapped reinforced column (UHGWRC)	150	450	01	-	GFRP wrapped sheet
Unheated CFRP wrapped reinforced column (UHCWRC)	150	450	01	-	CFRP wrapped sheet

Table 2. Mix proportion of concrete specimen

Cement (kg/m ³)	Water (kg/m ³)	Sand (kg/m ³)	Coarse aggregate(kg/m ³)
390	195	725	1088



Figure 1. Application of primer on column surface.



Figure 2 Application of putty on Column.

Table 3. Properties of primer

Aspect	Free flowing liquid
Mixed density	1.07 ± 0.02 kg/litre
Volume solids	100 %
Mixing ratio, by weight	100 (base): 50 (hardener)
Coverage	4 to 6 m ² /kg
Pot life	40 minutes at 25°C
Tack free time	6 hours at 25°C
	3 hours at 40°C
Adhesive bond strength to concrete	> 2.5 MPa

Table 4 Properties for putty and saturant

Aspect	Grey viscous paste	Translucent glue liquid
Mixed density	1.85 kg/litre	1.10 ± 0.03 kg/litre
Mixing ratio, by weight	100 (base): 75(hardener)	100 (base): 40(hardener)
Pot life	50 minutes at 25°C	25 minutes at 25°C
	30 minutes at 40°C	30 minutes at 40°C
Setting time	12 hours at 25°C	< 3 hours at 25°C
		< 4 hours at 40°C
Compressive strength	40 MPa at 24 hours	> 40 MPa at 1day
	65 MPa at 7 days	> 60 MPa at 7 days
Flexural strength	20 MPa at 7 days	> 35 MPa
Tensile strength	10 MPa at 7 days	> 17 MPa
Adhesive bond strength to concrete	2 MPa at 7 days	-

Table 5 Properties of CFRP and GFRP sheet

	CFRP	GFRP
Type of sheet	Carbon fibre, 430 gsm	E-Glass, 900 gsm
Modulus of elasticity	240 kN/mm ²	73 kN/mm ²
Tensile strength	3800 N/mm ²	3400 N/mm ²
Total weight of sheet	400 g/m ²	900 g/m ²
Density	1.7 g/cm ³	2.6 g/cm ³
ζ Ultimate	1.55	4.5
Thickness of static design	0.234 mm	0.342 mm
Weight/density		

2.7 Instruments and measurements

The experimental investigation evaluated thirty Reinforced Concrete (RC) columns subjected to axial compression tests using a Universal Testing Machine (UTM) in a laboratory environment. The specimens were loaded uniaxially through hydraulic pressure using a calibrated jack, enabling the measurement and analysis of their structural behavior under a compressive load.

To measure the displacement and strain of the column specimens, researchers used a displacement dial gauge and an electrical strain gauge, respectively. A displacement dial gauge was set up to contact the

desired measurement point and to monitor the column displacement as a load was applied. The demountable mechanical strain gauge (DEMEC) consists of a digital dial gauge attached to an Invar bar, featuring a fixed conical point at one end and a pivoting conical point on a knife edge at the other. The dial gauge measures the pivoting movement. Stainless-steel discs, pre-drilled and adhered to the structure, were positioned using a setting out bar to convert strain changes into dial gauge readings. The Model P3 Strain Indicator and Recorder are portable battery-operated devices that can accept four inputs from various strain gauge circuits, including strain gauge-based transducers. It functions as a bridge

amplifier, static strain indicator, and a digital data logger. The device is configured through a menu-driven interface for various measurement parameters, such as input and output channels, bridge configuration, measurement units, bridge balance, calibration method, and recording options. Data were recorded at a maximum rate of one reading per channel per second, stored on a removable multimedia card, and transferred to a computer via the USB. The device features a stable measurement circuit, regulated bridge excitation supply, and adjustable gauge factor, allowing measurements with 0.11 micro-strain resolution. For quarter-bridge operation, built-in bridge completion resistors of 120, 350, and 1000 Ω are available.



Figure 3 Application of saturant on column surface

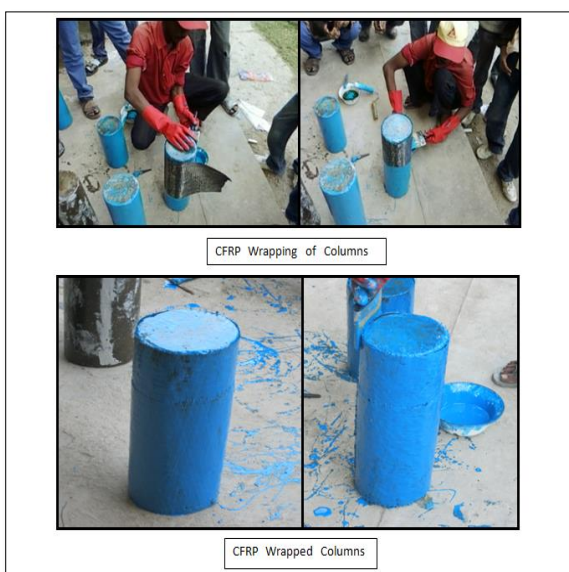


Figure 4 Application of CFRP sheet



Figure 5 Application of GFRP sheet

3. Results and Discussion

The experimental outcomes were compared for various concrete compositions, including fibre-reinforced, unwrapped, and wrapped reinforced concrete (RC) columns. The specimens were subjected to cyclical heat exposure at 200 °C for 6 hours per day over 75 cycles. The study assessed several crucial factors, such as the ultimate load capacity (failure load), load-displacement behavior, stress-strain characteristics, secant modulus, failure mechanisms, and cracking patterns.

3.1 Failure load

3.1.1 Failure load for fibre reinforced columns

Figure 6 illustrates a comparative analysis of the failure loads for the fibre-reinforced column specimens (150 x 300 mm² (D x H)) subjected to 75 cycles at 200 °C. The results indicate that HRC exhibited a 10.42% decrease in failure load compared to UHRC. HSFRFC demonstrated a 23.26% increase in failure load relative to HRC. In contrast, HHFRFC and HPPFRFC showed decreases of 34.88% and 32.56%, respectively, compared with HRC. Compared to HSFRFC, HHFRFC and HPPFRFC exhibited significant decreases in failure loads of 47.17% and 45.28%, respectively. HPPFRFC displayed a marginal increase of 3.57% in the failure load compared with the HHFRFC.

For specimens with dimensions of (150 x 450 mm² (D x H)), the failure load of the HRC decreased by 11.11% compared with that of the UHRC. HSFRFC showed a 27.5% increase in failure load relative to HRC, whereas HHFRFC and HPPFRFC exhibited decreases of 32.5% and 52.5%, respectively. Compared with HSFRFC, HHFRFC and HPPFRFC demonstrated substantial

decreases in failure loads of 47.06% and 62.75%, respectively. The HPPFRC exhibited a 29.63% decrease in the failure load compared with the HHFRC.

Table 6 Failure load for fibre reinforced concrete specimens

Specimen size (D = diameter, H = height)	Specimen type	Failure load (kN)	Average failure load (kN)
150 x 300 mm ² (D x H)	UHRC1	500	480
	UHRC2	460	
	HRC1	420	430
	HRC2	440	
	HSFRC1	520	530
	HSFRC2	540	
	HHFRC1	280	280
	HHFRC2	280	
	HPPFRC1	300	290
	HPPFRC2	280	
150 x 450 mm ² (D x H)	UHRC1	440	450
	UHRC2	460	
	HRC1	380	400
	HRC2	420	
	HSFRC1	520	510
	HSFRC2	500	
	HHFRC1	280	270
	HHFRC2	260	
	HPPFRC1	180	190
	HPPFRC2	200	

Table 7 Failure load for FRP wrapped concrete specimens

Specimen size	Specimen type	Failure load (kN)	Average failure load (kN)
150 x 300 mm ² (D x H)	UHRC1	500	480
	UHRC2	460	
	HRC1	420	430
	HRC2	440	
	HGWRC1	740	720
	HGWRC2	700	
	HCWRC1	600	590
	HCWRC1	580	
150 x 450 mm ² (D x H)	UHRC1	440	450
	UHRC2	460	
	HRC1	380	400
	HRC2	420	
	UHGWRC1	680	680
	UHCWRC1	780	780
	HGWRC1	620	630
	HGWRC2	640	
	HCWRC1	580	590
	HCWRC2	600	

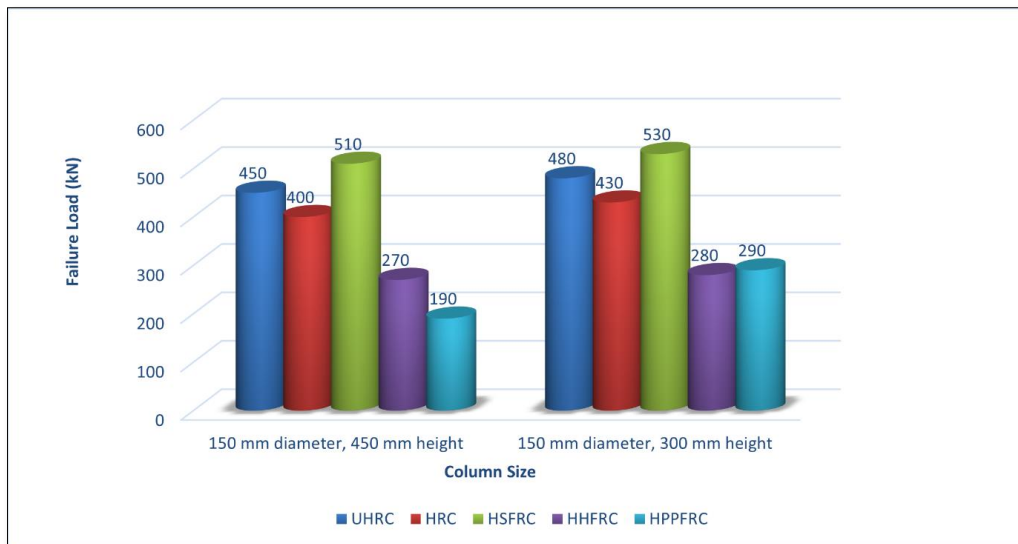


Figure 6 Failure load for fibre reinforced columns

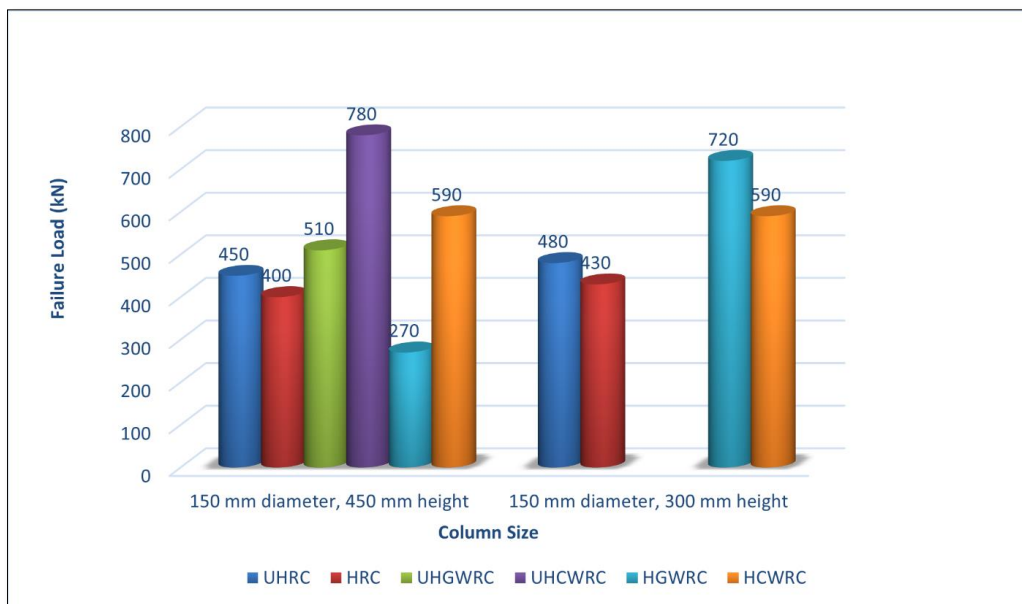


Figure 7 Failure load for FRP wrapped reinforced columns

The impact of the aspect ratio variation from 2 (150 x 300 mm² (D x H)) to 3 (150 x 450 mm² (D x H)) on the failure load was observed across different concrete types. The decrease in the failure load for the HRC compared with the UHRC changed from 10.42% to 11.11%. For HSFRC, compared to HRC, the increase in the failure load shifted from 23.26% to 27.5%. The decrease in failure load for HHFRC compared to HRC changed from 34.88% to 32.5%, whereas for HPPFRC compared to HRC, it increased from 32.56% to 52.5%. The decrease in the failure load for HHFRC compared to HSFRC remained relatively constant (47.17% to 47.06%), whereas for HPPFRC compared to HSFRC, it increased from 45.28% to 62.75%. Finally, the change in failure load for HPPFRC compared to HHFRC shifted from a 3.57% increase to a 29.63% decrease. Based on previous studies [13, 29] and current investigation, it was

found that HSFRC achieved a higher failure load than HPPFRC, HHFRC, HRC, and UHRC, but HHFRC and HPPFRC have lower failure loads than UHRC and HRC.

3.1.2 Failure load for FRP wrapped columns

Figure 7 presents a comparison of the failure loads for FRP-wrapped column specimens (150 x 300 mm² (D x H)) after 75 cycles at 200 °C. The failure load increased by 50% for the HGWRC and 22.92% for the HCWRC, compared to the UHRC. Additionally, the failure load increased by 67.44% for HGWRC and 37.21% for HCWRC, compared with HRC. Conversely, a decrease of 18.06% in the failure load was observed for the HCWRC compared with the HGWRC.

For the FRP-wrapped column specimens (150 x 450 mm² (D x H)) after 75 cycles at 200 °C, the failure load increased by 51.11% for UHGWR, 73.33% for UHCWR, 40% for HGWR, and 31.11% for HCWR compared to UHRC. Compared with HRC, the failure load increased by 70% for UHGWR, 95% for UHCWR, 57.5% for HGWR, and 47.5% for HCWR. When compared to UHGWR, the failure load increased by 14.71% for UHCWR, while it decreased by 7.35% for HGWR, and 13.24% for HCWR. Compared to the UHCWR, the failure load decreased by 19.23% for the HGWR and 24.36% for the HCWR. Additionally, an increase of 6.35% in the failure load was observed for the HCWR compared with the HGWR.

When the aspect ratio was increased from 2 (150 x 300 mm² (D x H)) to 3 (150 x 450 mm² (D x H)), the failure load changes were as follows: an increase from 50% to 40% for HGWR compared with UHRC, an increase from 22.92% to 31.11% for HCWR compared with UHRC, an increase from 67.44% to 57.5% for HGWR compared with HRC, an increase from 37.21% to 47.5% for HCWR compared with HRC, and a decrease from 18.06% to 6.35% for HCWR compared with HGWR. From the previous literature [19, 30] and our present work, we noticed that FRP-wrapped reinforced columns displayed a stronger capacity to tolerate failure loads than their unwrapped counterparts when exposed to elevated temperatures.

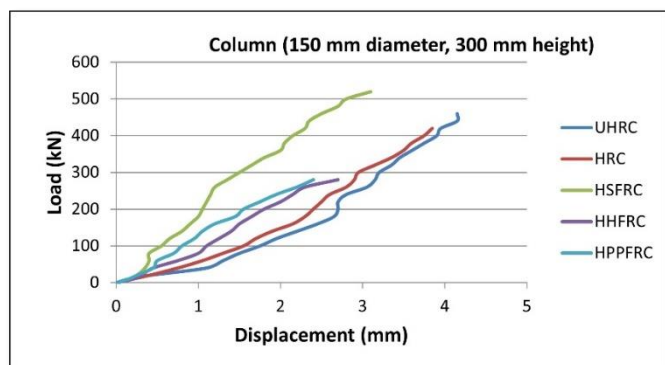


Figure 8 Load vs. displacement for fibre reinforced columns

3.2 Load vs. displacement

3.2.1 Load vs. displacement for fibre reinforced column

Figure 8 presents a comparison of the displacement for fibre-reinforced column specimens (150 x 300 mm² (D x H)) subjected to 75 cycles at 200 °C. A decrease in displacement of 7.23% was observed for the HRC column specimens compared to that of the UHRC. Furthermore, the displacement reductions for the HSFRC, HHFRC, and HPPFRC column specimens compared with HRC were 19.48%, 29.87%, and 37.66%, respectively. When comparing the HSFRC to the HHFRC and HPPFRC, the displacement reductions were 12.90% and 22.58%, respectively. In addition, the

displacement reduction of HPPFRC column specimens compared with HHFRC was 11.11%.

Figure 9 shows comparative displacement for fibre-reinforced column specimens (150 x 450 mm² (D x H)) after being subjected to 75 cycles to 200 °C, where it was found that the HRC specimen gave an increase in 19.13% displacement over UHRC specimen. In contrast, the HSFRC, HHFRC, and HPPFRC specimens demonstrated reductions in displacement of 33.58%, 14.60%, and 73.72%, respectively, compared to HRC. Further analysis revealed that the HHFRC specimens showed a 28.57% increase in displacement, whereas the HPPFRC specimens exhibited a 60.44% decrease in displacement relative to HSFRC. In addition, the displacement of the HPPFRC specimens was 69.23% lower than that of the HHFRC specimens. These findings suggest that fibre reinforcement significantly influences the displacement behavior of column specimens subjected to cyclic thermal loading.

The findings showed that there were notable variations in the displacement across different types of concrete when the aspect ratio was increased from 2 (150 x 300 mm² (D x H)) to 3 (150 x 450 mm² (D x H)). The displacement for the HRC dropped from 7.23% to 19.13% as compared to the UHRC. HSFRC exhibited a reduction from 19.48% to 33.58% compared to the HRC. HHFRC decreased from 29.87% to 14.60% relative to HRC. The most substantial reduction was observed in HPPFRC, with a decrease from 37.66% to 73.72% compared with HRC. When comparing fibre-reinforced concretes, HHFRC demonstrated a decrease from 12.90% to 28.57% relative to HSFRC, whereas HPPFRC showed a reduction from 22.58% to 60.44% compared to HSFRC. Finally, the HPPFRC exhibited a decrease from 11.11% to 69.23% compared to the HHFRC. These findings suggest that the aspect ratio and concrete composition significantly influence displacement characteristics. Fiber reinforced columns show less displacement compared to control columns at 200 °C. The findings presented here are also supported by previous studies [31, 32].

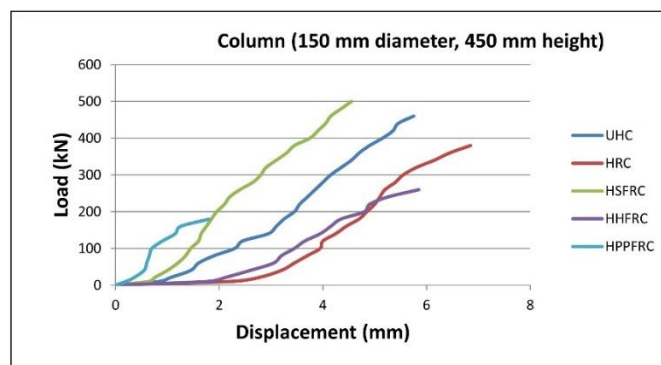


Figure 9 Load vs. displacement for fibre reinforced columns

3.2.2 Load vs. displacement for FRP wrapped columns

Figure 10 illustrates the comparative displacement analysis of the FRP-wrapped column specimens (150 x 300 mm² (D x H)) subjected to 75 cycles of thermal exposure at 200 °C. The results indicated significant variations in displacement across different specimen types. HGWRC exhibited a 135.07% increase in displacement relative to the UHRC, whereas the HCWRC showed a modest 5.85% increase. Compared to HRC, HGWRC and HCWRC demonstrated displacement increases of 106.02% and 118.07%, respectively. Furthermore, the HCWRC displayed a 122.08% greater displacement than that of the HGWRC. These quantitative findings underscore the differential effects of thermal cycling on the displacement characteristics of various FRP-wrapped column configurations.

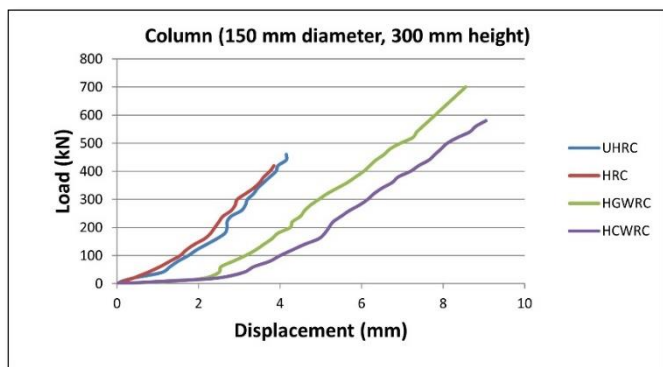


Figure 10 Load vs. displacement for FRP wrapped reinforced columns

Figure 11 presents a displacement comparison for FRP-wrapped column specimens (150 x 450 mm² (D x H)) subjected to 75 cycles at 200 °C. The results demonstrated significant variations in displacement among different concrete compositions. The UHWRC specimens exhibited the largest increase in displacement at 75.65%, followed by UHCWRC (51.30%), HGWRC (50.43%), and HCWRC (33.91%) compared to UHRC. When compared to the HRC, the displacement increases were 47.44% for UHWRC, 27% for UHCWRC, 26.28% for HGWRC, and 12.41% for HCWRC. Comparative analysis indicated displacement reductions in UHCWRC (13.86%), HGWRC (14.36%), and HCWRC (23.76%) relative to UHWRC. Additionally, the HGWRC and HCWRC showed minor displacement decreases of 0.57% and 11.49%, respectively, compared to the UHCWRC. HCWRC exhibited a 10.98% reduction in displacement relative to that of HGWRC. The observed reduction in the displacement can be attributed to the enhanced stiffness of the columns. Both heated and unheated FRP-wrapped columns demonstrated higher stiffness compared to their unwrapped counterparts, likely owing to the activation of GFRP and CFRP materials in the hoop direction.

When the aspect ratio was increased from 2 (150 x 300 mm² (D x H)) to 3 (150 x 450 mm² (D x H)), the displacement exhibited the following changes: an increase from 135.07% to 50.43% for HGWRC compared with UHRC, an increase from 5.85% to 33.91% for HCWRC compared with UHRC, an increase from 106.02% to 26.28% for HGWRC compared with HRC, an increase from 118.07% to 12.41% for HCWRC compared with HRC, and a decrease from 122.08% to 10.98% for HCWRC compared with HGWRC.

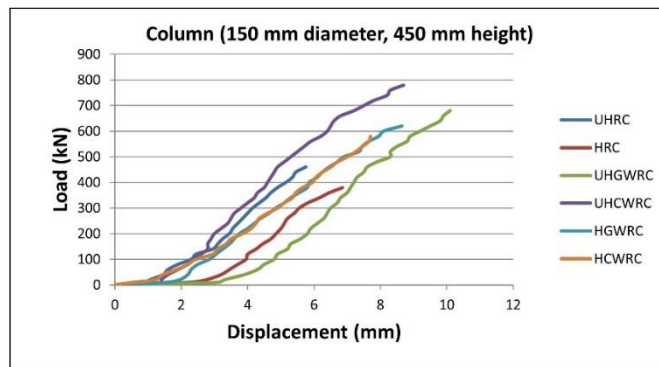


Figure 11 Load vs. displacement for FRP wrapped reinforced columns

3.3 Secant stiffness

The secant stiffness was calculated by dividing the peak compressive force by peak column displacement. Figure 12 illustrates the secant stiffness of reinforced columns (150 x 300 mm² (D x H)) encased with fibre and fibre-reinforced polymer (FRP). Figure 13 depicts the secant stiffness of reinforced columns (150 x 450 mm² (D x H)) encased with fibre and FRP.

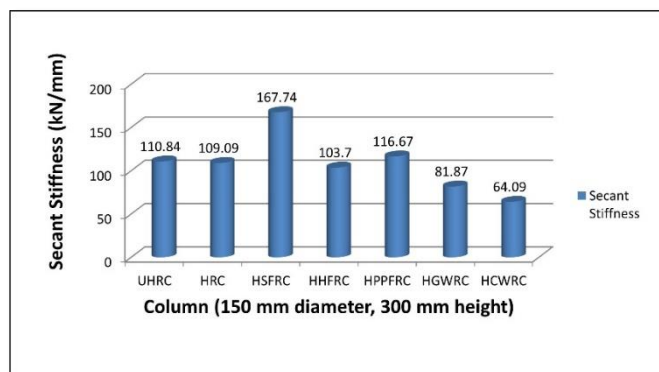


Figure 12 Secant stiffness of reinforced columns

3.4 Stress vs. strain relationship

Concrete strain is measured at three points in the columns, and FRP strain is recorded. The stress-strain relationships at the column center are considered most reliable, presented in Figures 14 to 17.

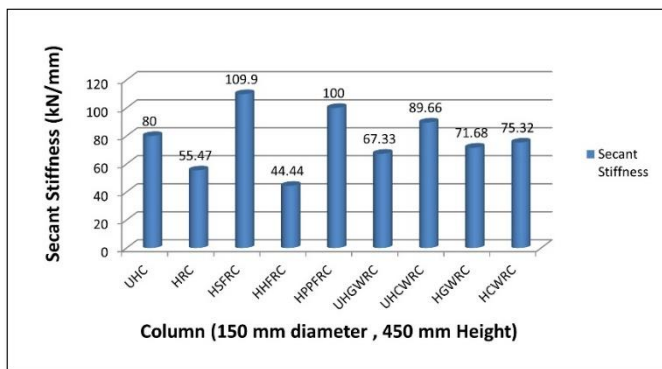


Figure 13 Secant stiffness of reinforced columns

3.4.1 Stress vs. strain relationship for fibre reinforced columns

Figure 14 presents the comparative strain analysis of the fibre-reinforced column specimens (150 x 300 mm² (D x H)) subjected to 75 cycles of thermal exposure at 200 °C. The results revealed significant variations in the strain behavior among different fibre-reinforced concrete compositions. HRC exhibited a 181.25% increase in strain compared to UHRC. Among the fibre-reinforced variants, HSFRC showed a 39.26% increase in strain relative to HRC, whereas HHFRC demonstrated a more substantial increase of 334.07%. In contrast, HPPFRC displayed a 31.11% reduction in strain compared with HRC. When comparing HSFRC to other fibre-reinforced compositions, HHFRC exhibited a 211.70% increase in strain, whereas HPPFRC exhibited a 50.53% decrease. Notably, the HPPFRC demonstrated the highest strain resistance, with an 84.13% reduction compared to that of the HHFRC. These findings suggest that the incorporation of polypropylene fibres may enhance the thermal strain resistance of concrete columns under cyclic high-temperature exposure.

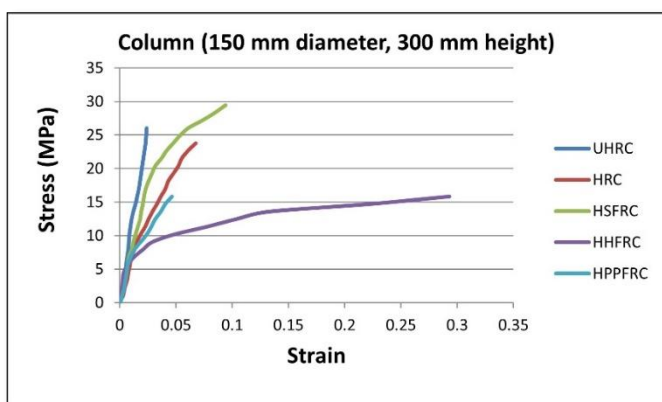


Figure 14 Stress vs. strain at mid-height of fibre reinforced columns

The results of the strain analysis for the fibre-reinforced column specimens (150 x 450 mm² (D x H)) after exposure to 75 cycles at 200 °C are presented in

Figure 15. Compared to the UHRC, the HRC exhibited a 68.61% decrease in strain. HSFRC showed a 37.24% decrease in strain relative to HRC, whereas HHFRC and HPPFRC demonstrated increases of 237.24% and 56.55%, respectively. Compared to HSFRC, HHFRC and HPPFRC displayed strain increases of 437.36% and 149.45%, respectively. Finally, HPPFRC exhibited a 53.58% decrease in strain compared with HHFRC. These findings indicate significant variations in strain behavior among different fibre-reinforced concrete compositions under cyclic thermal loading.

The results indicate that increasing the aspect ratio from 2 (150 x 300 mm² (D x H)) to 3 (150 x 450 mm² (D x H)) led to significant changes in the strain across various concrete types. For HRC, compared to UHRC, the strain decreased from 181.25% to 68.61%. HSFRC exhibited a slight decrease in strain relative to the HRC, from 39.26% to 37.24%. In contrast, HHFRC showed a substantial increase in strain compared with HRC, from 334.07% to 237.24%. HPPFRC also demonstrated an increase in strain relative to HRC, from 31.11% to 56.55%. When comparing the HHFRC to HSFRC, the strain increased from 211.70% to 437.36%. Compared to HSFRC, HPPFRC showed an increase in strain from 50.53% to 149.45%. Finally, HPPFRC exhibited a decrease in strain relative to that of HHFRC, from 84.13% to 53.58%.

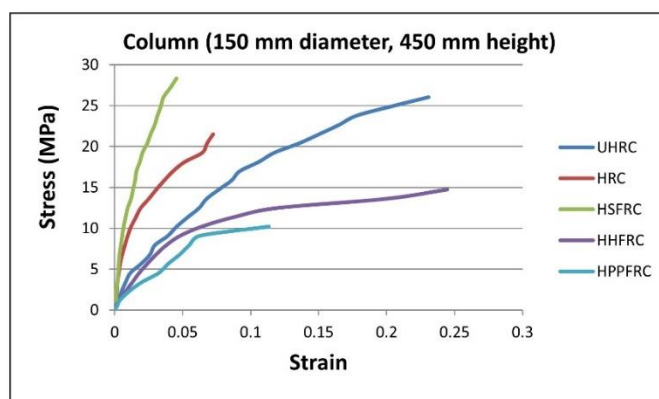


Figure 15 Stress vs. strain at mid-height of fibre reinforced columns

3.4.2 Stress vs. strain relationship for FRP wrapped columns

Figure 16 illustrates the strain comparison for the FRP-wrapped column specimens (150 x 300 mm² (D x H)) after exposure to 75 cycles at 200 °C. The results indicate that the HGWRFC specimens exhibited a 36.30% increase in strain compared to UHRC, whereas the HCWRFC specimens showed a 77.83% decrease in strain relative to UHRC. When compared to HRC, the HGWRFC specimens demonstrated a substantial 1629.17% increase in strain, whereas the HCWRFC specimens exhibited a 283.33% increase. These findings suggest significant variations in the strain

behavior among the different column types under high-temperature cyclic loading conditions.

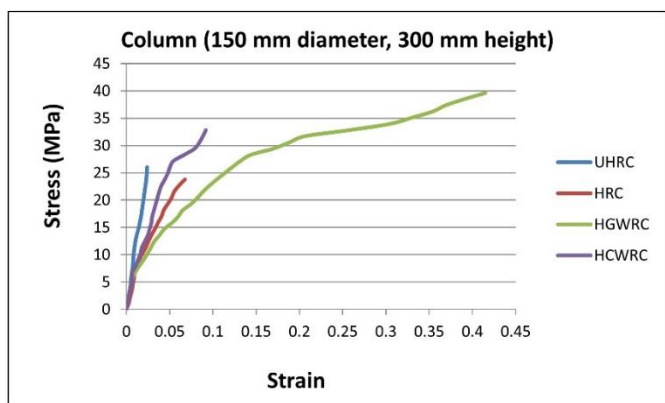


Figure 16 Stress vs. strain at mid-height of FRP wrapped columns

The strain behavior of the FRP-wrapped column specimens (150 x 450 mm² (D x H)) after exposure to 75 cycles at 200 °C is shown in Figure 17. Compared to UHRC, UHGWRC exhibited a 33.33% decrease in strain, whereas UHCWRC, HGWRC, and HCWRC showed increases of 123.81%, 56.93%, and 52.38%, respectively. Compared to HRC, strain increases were observed for UHGWRC (112.41%), UHCWRC (613.10%), HGWRC (400%), and HCWRC (51.72%). UHCWRC, HGWRC, and HCWRC demonstrated strain increases of 235.71%, 135.39%, and 28.57%, respectively, relative to UHGWRC. Compared to UHCWRC, HGWRC and HCWRC showed strain decreases of 29.88% and 78.72%, respectively. Finally, the HCWRC exhibited a 69.65% strain decrease compared to the HGWRC. These results indicate significant variations in the strain behavior among different concrete compositions when subjected to elevated temperature cycles.

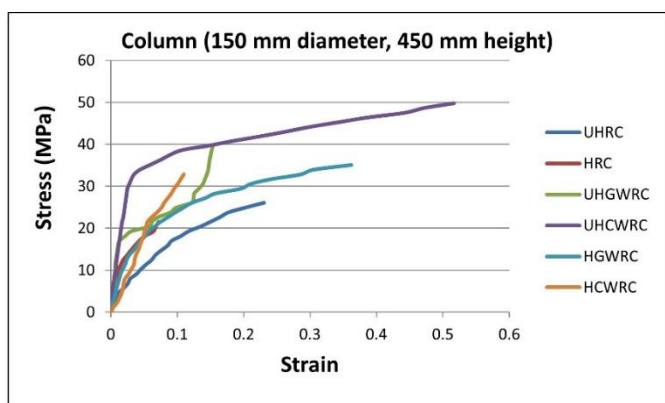


Figure 17 Stress vs. strain at mid-height of FRP wrapped columns

3.5 Failure mode and crack pattern

Figures 18-26 illustrate the crack patterns and failure modes exhibited by all the column specimens.

Each figure is structured into three parts: the initial section shows the column before failure, and the subsequent two sections depict the column after failure. These visual representations provided a comprehensive analysis of the structural behavior and damage progression of the tested samples. By examining the observed crack patterns and failure modes, researchers can gain valuable insights into the performance of columns and their load-bearing capabilities under the specific testing conditions employed.



Figure 18 Crack patterns and failure mode of UHRC



Figure 19 Crack patterns and failure mode of HRC

3.5.1 Fibres

The crack patterns and failure modes of various fibre-reinforced concrete specimens exposed to high temperatures are shown in Figures 18-22. These images indicate that cracks primarily spread in the radial direction across the circular cross-sections of the specimens. Moreover, the axial loading produced

longitudinal cracks that extended approximately 15 cm from the load application point. Interestingly, concrete spalling on the outer surface is visible in Figures 18 and 19, whereas only crack formation is observed in Figures 20-22. This distinction implies that incorporating fibres into the concrete mixture effectively reduces spalling when the material is subjected to high temperatures.

UHCWRC specimens experienced complete concrete crushing. The failure patterns depicted in Figures 23–26 is consistent across the samples [28]. UHWRC and UHCWRC-wrapped columns failed abruptly without warning signs. On the other hand, the HGWRC and HCWRC wrapped columns exhibited impending failure. The failure process of these specimens began with the rupture of a small bottom section of the column wrapping, followed by the gradual rupture of the remaining wrap. Failure was observed up to 100 mm in height in both HGWRC and HCWRC specimens, whereas cracks extended up to 300 mm in height in HRC specimens.



Figure 20 Crack patterns and failure mode of HSFRC



Figure 21 Crack patterns and failure mode of HHFRC

3.5.2 FRP wrapping

The crack patterns and failure modes of various FRP-wrapped columns subjected to high and normal room temperatures are shown in Figures 23–26. UHWRC and UHCWRC specimens failed because of the rupture of the GFRP and CFRP materials, respectively, when the tensile stresses surpassed their tensile strength. The 150 mm overlap likely prevented debonding in these specimens. In contrast, the UHRC specimens exhibited visible cracks, whereas the



Figure 22 Crack patterns and failure mode of HPPFRC



Figure 23 Crack pattern and failure mode UHWRC



Figure 24 Crack pattern and failure mode UHCWRC



Figure 25 Crack pattern and failure mode HGWRC



Figure 26 Crack pattern and failure mode HCWRC

4. Conclusion

Experimental investigations are conducted to study the change in behavior of fibre reinforced RC columns and FRP wrapped RC columns after applying 200 °C for a 6 hours per day over 75 cycles. Design of different size RC column is conducted using codal provisions of IS:456. The columns are designed for minimum reinforcement as per codal provisions where the required reinforcement is less. The columns are strengthened using 0.342 mm and 0.234 mm GFRP and CFRP sheets respectively. For axial loading conditions, experiments have been conducted on total thirty RC columns. Different structural parameters like ultimate load-carrying capacity (failure load), displacement, secant stiffness, strain, failure modes, and crack patterns are evaluated. Performance has been compared for heated reinforced column and fibre reinforced column, unheated reinforced columns and unheated, heated FRP wrapped reinforced columns before and after exposure to high temperature.

4.1 RC column specimens using fibres

- Higher failure load is observed for HSFRC as compared to HPPFRC, HHFRC, HRC and UHRC, whereas HHFRC and HPPFRC exhibited lower failure loads in comparison to UHRC and HRC. Increase in failure load is observed of 23.26% to 27.5% for HSFRC compared to HRC after applying 75 cycles of 200 °C temperature. Decrease in failure load is observed of 32.5% to 34.88% for HHFRC and 32.56% to 52.5% for HPPFRC compared to HRC at high temperature.
- Lesser displacement is observed for of fibre reinforced columns as compared to control columns exposed to 200 °C temperature. A decrease in displacement was observed from 19.48% to 33.58% for HSFRC, 14.60% to 29.87% for HHFRC, and 37.66% to 73.52% for HPPFRC compared to HRC after applying a high temperature.
- The secant stiffness of the HSFRC column was higher than that of the other fibre-reinforced columns exposed to high temperatures.
- Compared with the HRC, the column reinforced with steel fibres demonstrated a 37.24% strain decrease at its mid-height when exposed to a temperature of 200 °C.

4.2 RC column specimens strengthened using FRP

- FRP-wrapped reinforced columns demonstrated a greater capacity to withstand failure loads than their unwrapped counterparts when subjected to

elevated temperatures. The failure load increased by 51.11% for UHWRC, 73.33% for UHCWRC, 40% to 50% for HGWRC, and 22.92% to 31.11% for HCWRC compared to UHRC under high-temperature conditions. However, when compared to unheated FRP-wrapped reinforced columns, HGWRC exhibited a 7.35% decrease in failure load, whereas HCWRC showed a 23.36% reduction.

- Columns reinforced with FRP wrapping exhibited greater displacement than the control columns when subjected to elevated temperatures. The increase in displacement relative to UHRC under high-temperature conditions was measured at 75.65% for UHWRC, 51.30% for UHCWRC, 50.43% for HGWRC, and 33.91% for HCWRC.
- Compared with other FRP-wrapped columns subjected to elevated temperatures, the UHCWRC column exhibited greater secant stiffness.

At elevated temperatures, reinforced columns wrapped with FRP display increased strain at mid-height compared to untreated control columns. Furthermore, a strain reduction of 33.33% was noted in UHWRC compared to UHRC when exposed to high-temperature environments.

References

- [1] R.H. Haddad, R.J. Al-Saleh, N.M. Al-Akhras, Effect of elevated temperature on bond between steel reinforcement and fiber reinforced concrete. *Fire Safety Journal*, 43(5), (2008) 334–343. <https://doi.org/10.1016/j.firesaf.2007.11.002>
- [2] M.J. Alshannag, A. Alshenawy, Effective strengthening schemes for heat damaged reinforced concrete beams. *Journal of King Saud University - Engineering Sciences*, 32(4), (2020) 236–245. <https://doi.org/10.1016/j.jksues.2019.10.003>
- [3] T.T. Lie, V.K.R. Kodur, Thermal and mechanical properties of steel-fibre-reinforced concrete at elevated temperatures. *Canadian Journal of Civil Engineering*, 23, (1996) 511–517. <https://doi.org/10.1139/l96-055>
- [4] A.M. Tahwia, M. Mokhles, W.E. Elemam, Optimizing characteristics of high-performance concrete incorporating hybrid polypropylene fibers. *Innovative Infrastructure Solutions*, 8(297), (2023). <https://doi.org/10.1007/s41062-023-01268-6>
- [5] P. Kalifa, G. Chéné, C. Gallé, High-temperature behaviour of HPC with polypropylene fibres: From spalling to microstructure. *Cement and Concrete Research*, 31(10), (2001) 1487–1499. [https://doi.org/10.1016/S0008-8846\(01\)00596-8](https://doi.org/10.1016/S0008-8846(01)00596-8)
- [6] J.D. Ríos, H. Cifuentes, C. Leiva, C. García, M.D. Alba, Behavior of High-Strength Polypropylene Fiber-Reinforced Self-Compacting Concrete Exposed to High Temperatures. *Journal of Materials in Civil Engineering*, 30(11), (2018) 04018271. [https://doi.org/10.1061/\(ASCE\)MT.1943-5533.0002491](https://doi.org/10.1061/(ASCE)MT.1943-5533.0002491)
- [7] M. Mubarak, R.S.M. Rashid, M. Amran, R. Fediuk, N. Vatin, S. Klyuev, Mechanical properties of high-performance hybrid fibre-reinforced concrete at elevated temperatures. *Sustainability (Switzerland)*, 13(23), (2021) 13392. <https://doi.org/10.3390/su132313392>
- [8] R.H. Ahmed, G.D. Abdel-Hameed, A.M. Farahat, Behavior of hybrid high-strength fiber reinforced concrete slab-column connections under the effect of high temperature. *HBRC Journal*, 12(1), (2016) 54–62. <https://doi.org/10.1016/j.hbrcj.2016.01.007>
- [9] Y. Li, X. Liu, M. Wu, Mechanical properties of FRP-strengthened concrete at elevated temperature. *Construction and Building Materials*, 134, (2017) 424–432. <https://doi.org/10.1016/j.conbuildmat.2016.12.148>
- [10] A.C.S. Bezerra, P.S. Maciel, E.C.S. Corrêa, P.R.R. Soares Junior, M.T.P. Aguiar, P.R. Cetlin, Effect of high temperature on the mechanical properties of steel fiber-reinforced concrete. *Fibers*, 7(12), (2019) 100. <https://doi.org/10.3390/fib7120100>
- [11] B. Roy, A.S.M. Akid, Md.H.R. Sobuz, J. Shuvra, Md.S. Islam, Experimental investigation on mechanical performance of high-strength concrete containing polypropylene fiber exposed to high temperature. *Asian Journal of Civil Engineering*, 22, (2021) 1595–1606. <https://doi.org/10.1007/s42107-021-00399-4>
- [12] H. Jianqiang, W. Qing, Y. Boyu, H. Johnny, Impact of Elevated Temperatures on the Performance of High-Strength Engineered Cementitious Composite. *Journal of Materials in Civil Engineering*, 33(9), (2021) 04021222. [https://doi.org/10.1061/\(ASCE\)MT.1943-5533.0003812](https://doi.org/10.1061/(ASCE)MT.1943-5533.0003812)
- [13] I. Banoth, A. Agarwal, Bond between deformed steel rebars and concrete at elevated temperatures. *Fire Safety Journal*, 145, (2024) 104133. <https://doi.org/10.1016/j.firesaf.2024.104133>
- [14] N. Kabashi, E. Krasniq, M. Muhaxheri, F. Salihu, B. Gashi, High-Temperature Behaviour of Concrete with Polypropylene Fibres. In *Proceedings of 5th International Conference on Civil Engineering and Architecture*, T. Kang (Ed.), Springer Nature Singapore, Singapore, (2024) 47–55.
- [15] T. Trapko, The effect of high temperature on the performance of CFRP and FRCM confined concrete elements. *Composites Part B*, 54(1),

- (2013) 138–145.
<https://doi.org/10.1016/j.compositesb.2013.05.016>
- [16] N. Moghtadernejad, M. Jamshidi, M.R. Maheri, C.K. Keong, Repair of post-heated short rectangular reinforced concrete columns with FRP jackets. *Structures*, 34, (2021) 4269–4283.
<https://doi.org/10.1016/j.istruc.2021.10.038>
- [17] Y.X. Liew, N. Bakar, K.S. Lim, S.I. Doh, R.P. Jaya, S.C. Chin, Shear Strengthening of Reinforced Concrete Beams using GFRP. *The Open Civil Engineering Journal*, 16(1), (2022).
<https://doi.org/10.2174/18741495-v16-e221222-2022-53>
- [18] H.S. Al-Nimry, A.M. Ghanem, FRP Confinement of Heat-Damaged Circular RC Columns. *International Journal of Concrete Structures and Materials*, 11(1), (2017) 115–133.
<https://doi.org/10.1007/s40069-016-0181-4>
- [19] D.S. Vijayan, A. Mohan, J.J. Daniel, V. Gokulnath, B. Saravanan, P.D. Kumar, Experimental Investigation on the Ecofriendly External Wrapping of Glass Fiber Reinforced Polymer in Concrete Columns. *Advances in Materials Science and Engineering*, 2021(1), (2021) 2909033.
<https://doi.org/10.1155/2021/2909033>
- [20] T.S. Mohammad, F.K. Karim, Strengthening of Concrete Columns under Axial Loading Condition with FRP. *American Journal of Engineering Research (AJER)*, 9(3), (2020) 6–16.
- [21] W. Zheng, B. Luo, Y. Wang, Microstructure and mechanical properties of RPC containing PP fibres at elevated temperatures. *Magazine of Concrete Research*, 66(8), (2014) 397–408.
<https://doi.org/10.1680/mac.13.00232>
- [22] Y.A. Al-Salloum, H.M. Elsanadedy, A.A. Abadel, Behavior of FRP-confined concrete after high temperature exposure. *Construction and Building Materials*, 25(2), (2011) 838–850.
<https://doi.org/10.1016/j.conbuildmat.2010.06.103>
- [23] M. Bazli, M. Abolfazli, Mechanical Properties of Fibre Reinforced Polymers under Elevated Temperatures: An Overview. *Polymers (Basel)*, 12(11), (2020).
<https://doi.org/10.3390/polym12112600>
- [24] IS 383:2016. Coarse and fine aggregate for concrete—specification (Third Revision).
- [25] IS 12269:2013. Ordinary Portland Cement 53 grade—specification.
- [26] IS 10262:2009. Indian concrete mix design guidelines (2009).
- [27] BIS (Bureau of Indian Standards), Plain and reinforced concrete: code of practice. IS 456, (2000).
- [28] S.W. Yoo, J.F. Choo, Behavior of CFRP-reinforced concrete columns at elevated temperatures. *Construction and Building Materials*, 358, (2022) 129425.
<https://doi.org/10.1016/j.conbuildmat.2022.129425>
- [29] M. Elsayed, M. Abou Elmaaty, R. Mohamed, Retrofitting of post-heated R.C. columns using steel fiber reinforced self-compacting concrete jackets. *Construction and Building Materials*, 400, (2023) 132637.
<https://doi.org/10.1016/j.conbuildmat.2023.132637>
- [30] F. Sharifianjazi, P. Zeydi, M. Bazli, A. Esmaeilkhanian, R. Rahmani, L. Bazli, S. Khaksar, Fibre-Reinforced Polymer Reinforced Concrete Members under Elevated Temperatures: A Review on Structural Performance. *Polymers (Basel)*, 14(3), (2022) 472.
<https://doi.org/10.3390/polym14030472>
- [31] L. Xiao, P. Chen, J. Huang, S. Peng, Z. Yang, Compressive behavior of reinforced steel-PVA hybrid fiber concrete short columns after high temperature exposure. *Construction and Building Materials*, 342, (2022) 127935.
<https://doi.org/10.1016/j.conbuildmat.2022.127935>
- [32] H. Elsanadedy, T. Almusallam, Y. Al-Salloum, R. Iqbal, Effect of high temperature on structural response of reinforced concrete circular columns strengthened with fiber reinforced polymer composites. *Journal of Composite Materials*, 51(3), (2017) 333–355.
<https://doi.org/10.1177/0021998316645171>

Authors Contribution Statement

Maulik Mistry: Writing – Original draft, Project administration, Visualization, Validation, Methodology design, Resource acquisition, Investigation, Conceptualization. Prasad Barve: Writing – review & editing, Visualization, Validation, Methodology design, Data analysis and interpretation, Conceptualization. Piyush Patel: Writing – review & editing, Visualization, Validation, Supervision, Project administration, Conceptualization. All authors have read and approved the final version of the manuscript.

Funding

The authors declare that no funds, grants or any other support were received during the preparation of this manuscript.

Competing Interests

The authors declare that there are no conflicts of interest regarding the publication of this manuscript.

Data Availability

The data supporting the findings of this study can be obtained from the corresponding author upon reasonable request.

Has this article screened for similarity?

Yes

About the License

© The Author(s) 2025. The text of this article is open access and licensed under a Creative Commons Attribution 4.0 International License.